European Journal of Agriculture and Food Sciences
Vol 6 | Issue 5 | October 2024
ISSN 2684-1827

RESEARCH ARTICLE

Research on Deposition Characteristics of a New Air-Assisted Electrostatic Sprayer

Liangfu Zhou* and Binbin Zhou

ABSTRACT

This study evaluated the properties of a new double air-assisted electrostatic orchard sprayer, focusing particularly on the impact of its electrostatic system on droplet deposition. The sprayer featured 10 nozzles, a centrifugal fan, and an axial fan, with an overall flow rate of 3.5 L/min and nozzle air velocities of 25 m/s (interior) and 12.5 m/s (exterior). Droplet sampling was conducted using paper cards and ponceau solution as a tracer. Field measurements in a Y-tree trained pear orchard assessed the effects of tractor speeds (0.34, 0.52, 0.84, and 1.05 m/s) and sampling positions (exposed and hidden faces). Tractor speed did not significantly affect overall droplet density, but the normalized droplet density on the exposed face increased with speed, while it decreased on the hidden face. The average normalized droplet density at all speeds was approximately 114.6 dot/cm^2. The electrostatic system improved droplet deposition on the hidden face of leaves, particularly on the side of the tree near the sprayer. The coefficient of variation (CV) of the exposed face increased with tractor speed, while tractor speed had no impact on the CV of the hidden face. Overall, the electrostatic system reduced the CV. This research offers valuable insights into the use of electrostatic sprayers.

Keywords: Air-assisted spraying, Electrostatic spraying, Orchard sprayer, Plant protection machine.

Submitted: August 30, 2024
Published: October 22, 2024

10.24018/ejfood.2024.6.5.862

Nanjing Vocational University of Industry Technology, China.

Corresponding Author:
e-mail: 2020101069@niit.edu.cn

1. Introduction

Air-assisted spraying is effective for transporting and depositing droplets onto crop canopies due to the airflow generated by the fan [1]. In China, fruit tree sprayers typically combine a spraying system with a fan to direct pesticide droplets into the canopy, aiming to match airflow and spray volume with canopy characteristics to minimize pesticide use, ensure even distribution, and prevent migration [2], [3]. Electrostatic spraying has been reported as highly effective for enhancing droplet deposition efficiency [4], [5], particularly on hidden leaf surfaces [6], [7]. Studies comparing electrostatic sprayers to traditional multi-row sprayers in pergola vineyards have demonstrated that electrostatic sprayers can reduce application volume by up to 68% while achieving similar or better droplet distribution throughout the canopy [8], [9]. However, despite its effectiveness in industrial applications, agricultural electrostatic spraying faces challenges in charging and transporting droplets deep into canopies under outdoor conditions.

Research has consistently shown that charged droplets improve total deposition [10]–[12]. For instance, Simone and Emanuele [13] found that electrostatic spraying increased droplet deposition on the back of leaves by an average of 44%. Although sampling location affects results, tractor speed does not significantly alter normalized spray deposition [14]. Studies by Cerruto also noted no significant impact of tractor speed on normalized deposition but observed an increase in coefficient of variation (CV) from 107% at 5 km/h to 121% at 6 km/h [15]. Additionally, Dong-Bin developed a novel evaluation method using fluorescent tracers, which revealed a 67% increase in normalized droplet deposition on the back of a cylinder for charged droplets [16].

This paper evaluates the effect of electrostatic spraying on droplet deposition in the canopy of Y-shaped pear trees using an innovative double air-assisted electrostatic sprayer, comparing results to non-electrostatic spraying with the same sprayer.

2. Materials and Methods

According to international standard ISO 5686-2, the description of sprayer settings should include details on the sprayer itself, nozzles, liquid distribution, and airflow distribution.

2.1. The Electrostatic Sprayer

The field trials utilized a trailed sprayer equipped with a double air-assisted electrostatic spraying system and a 400 L tank, which represents a newer model compared to those currently used in orchards [17]. This electrostatic sprayer employs an induction method for charging droplets and a double air-assisted system to deliver the charged droplets onto the canopy.

The sprayer features a hydraulic system comprising a hydraulic pump and three hydro-motors that separately drive the centrifugal fan, axial fan, and diaphragm pump. The hydraulic pump, powered by the tractor's power take-off (PTO), connects to a distribution valve that drives the centrifugal fan to generate interior airflow (airflow into the nozzle) to counteract electrostatic forces, as well as to the axial fan for droplet transport and the diaphragm pump for delivering pesticide solutions from the tank. The output of the centrifugal fan is routed through hoses to the 10 nozzles. The power transmission system is illustrated in Fig. 1.

To achieve high performance, the designer recommends setting the sprayer to a spraying pressure of 0.5 MPa, as indicated by a pressure gauge mounted at the nozzle's front end, with adjustments possible via a return valve. The total flow rate is 3.5 L/min, with each nozzle delivering 0.35 L/min. Under these conditions, the droplet volume median diameter (VMD) ranges from 110 to 130 μm. During testing, the operator must maintain the engine at full throttle to ensure consistent pressure and tractor speed.

2.2. Air-Assisted Electrostatic Nozzle

The electrostatic nozzle is the key component of the sprayer, featuring an electrode mounted at the nozzle's front. The interior airflow and spray liquid enter the nozzle separately (Fig. 2). The liquid is atomized into droplets under pressure from the diaphragm pump, then electrostatically charged by induction and carried to the canopy by the airflow generated by the centrifugal fan.

The brass electrode is installed in the nozzle cap, which is made from insulating material and positioned close to the nozzle outlet. This setup aims to achieve a stronger electric field gradient at a lower induced voltage, allowing more free electrons to be transferred to the droplets. This nozzle can achieve a charge-to-mass ratio (CMR) ranging from 0.8 to 1.2 mC/kg with an electrode voltage of 6 kV.

In this context, the dynamic behavior of charged droplets in the air field must be considered. The primary forces acting on the droplets include gravity, drag force from airflow, and the electromotive force from the electrostatic field. The electrostatic and drag forces are crucial for determining the droplet deposition path [18]–[20]. Therefore, the variation in droplet velocity can be calculated using the following (1):

$$\frac{du_p}{dt} = F_D \cdot (u - u_p) - q \cdot E \tag{1}$$

where u_p is the droplet velocity, m/s; F_D is the coefficient of drag force, N; u is the air velocity, m/s; q is the charge of droplet, C; E is the electric intensity, V/m.

Furthermore, the droplet velocity u_p at the outlet of nozzle can be calculated by the following (2):

$$u_p = \frac{4Q}{\pi \varphi^2} \tag{2}$$

where Q is flowrate for each nozzle, L/min; Φ is diameter of nozzle hole, $\Phi = 0.8$ mm $Q = 0.35$ L/min. So the droplet velocity can be calculated by the (2) $u_p = 11.6$ m/s.

From (1), it is clear that the electromotive force near the nozzle is directed toward the electrode, while the drag force acts towards the target, provided the air velocity exceeds the droplet velocity. Therefore, it is crucial to adjust the interior air velocity to exceed 11.6 m/s to ensure that the charged droplets are effectively transferred to the tree canopy.

2.3. Measure of Nozzle Flow Rate

A graduated cylinder is used to measure the total amount of liquid delivered by each nozzle over a 1-minute spraying period. The average of three measurements is calculated to determine the result. The nozzles are arranged with bilateral symmetry and are numbered from No. 1 to No. 5, starting with the lowest nozzle furthest from the center of the sprayer. For more accurate results, the double air jets are turned off during the measurement.

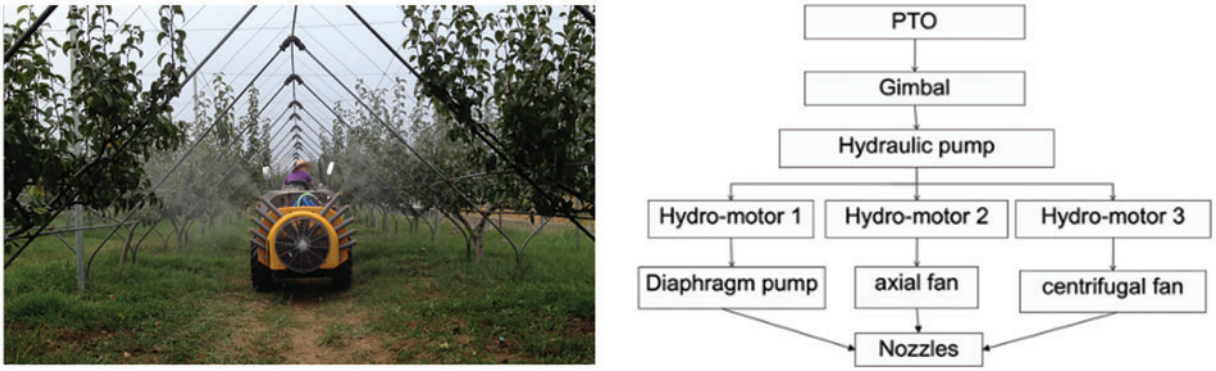

Fig. 1. Transmission system.

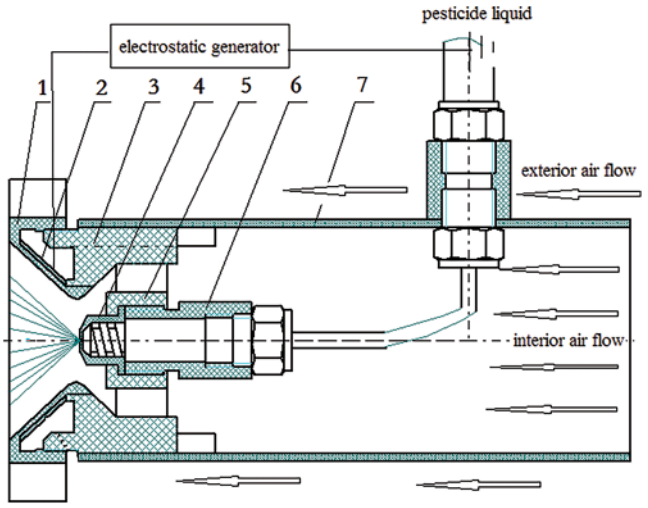

Fig. 2. Schematic diagram of nozzle structure.

The experiments were conducted at the recommended pressure of 0.5 MPa, consistent with field tests. Flow rates and positions for each nozzle are detailed in Table I. Results indicate that the flow rate error was less than ±2.5%, with an average discharge rate of 0.35 L/min. According to standard testing methods, deviations for each nozzle were within 2% of the average flow rate.

2.4. The Orchard and Canopy

The experiments were conducted in a "Y"-shaped pear orchard on a demonstration plot, a popular area for the fruit industry. The 50 m × 50 m experimental plot is a modern pear orchard with a 4 m wide accommodation road for agricultural machinery. Throughout the period from April to November, 6–8 treatments were applied. The spray gun used typically applies pesticides at high volumes exceeding 1000 L/ha with coarse droplets larger than 600 μm. The orchard features a Y-type pipe frame and steel wire at varying heights to guide tree growth. The trees, five years old, are planted with a row spacing of approximately 5 m × 4 m.

2.5. The Experiment Design

Environmental parameters such as temperature, wind velocity, and relative humidity were monitored during the tests. Spray treatments were conducted at four forward speeds: 0.34 m/s, 0.52 m/s, 0.84 m/s, and 1.05 m/s. To assess the impact of the electrostatic spraying system on canopy deposition and airborne drift at different speeds, the system was alternately switched on and off. Throughout the tests, spray pressure and fan rotation rates remained constant. The spray pressure was set to 0.5 MPa, yielding a spray volume of 3.5 L/min. The centrifugal fan and axial fan rotated at 1450 and 1800 r/min, respectively, resulting in outlet air velocities of 25 and 12.5 m/s. The average air temperature was 26°C, relative humidity was 57.5%, and wind speed averaged 2.3 m/s. Other operational parameters are listed in Table II.

TABLE I: Nozzle Characteristics and Position

No.	Right nozzle			
	Flow rate/ ($L \cdot min^{-1}$)	Nozzle height/mm	Distance to tree axis/mm	Direction/(°)
1	0.357 ± 0.025	650	650	15
2	0.344 ± 0.020	880	620	25
3	0.355 ± 0.025	1030	580	30
4	0.345 ± 0.024	1200	480	40
5	0.352 ± 0.023	1350	350	50

TABLE II: Parameters and Treatments

Parameter	Treatments					
	NO.1	NO.2	NO.3	NO.4	NO.5	NO.6
Tractor speed, m/s	0.34	0.52	0.52	0.84	1.05	1.05
Electrostatic system	ON	ON	OFF	ON	ON	OFF
Spraying pressure, MPa	0.5	0.5	0.5	0.5	0.5	0.5
Spray volume, L/min	3.5	3.5	3.5	3.5	3.5	3.5

The experiment aimed to evaluate the effects of tractor speed and the activation of the electrostatic system on droplet deposition onto the canopy and off-target. Each treatment trial was repeated three times at the same sample location. The canopy deposition experiment involved three adjacent rows, approximately 10 m wide. The sprayer applied pesticide liquid to the three inter-rows under real conditions, with the central inter-row designated as the experimental plot (Fig. 3). The spray mixture included a food dye tracer (Xylidine Ponceau 2R, produced by Beijing Chemical Reagent Factory) at a concentration of 5 g/L.

2.6. Sampling

In each replication, three trees were chosen to carry out the measurements of droplet deposition on canopy. The three target trees were selected in central of the row in order to keep enough trees in both end of the rows to prevent "start-up" and "finishing" effects.

A zone sampling strategy, commonly used to determine the overall distribution of tracer in the canopy, was employed for field measurements of spray distribution in tree and bush crops. This method averages leaf deposits physically, which can result in some loss of detailed information. For the height of the tree, three horizontal zones were defined at 0.9 m, 1.65 m, and 2.2 m. Given that the canopy width exceeds 50 cm, the vertical zones were categorized into three areas: two exterior zones (E_1, E_2) and one interior zone (I).

The sampling trees were divided into a total of nine zones (Fig. 4). Two sampling cards were used to collect data from both the exposed and hidden faces of each leaf. Three samples were collected from each exterior zone, and six samples from each interior zone. The representative random sampling method was employed, with positions tabbed to ensure consistency in duplicate tests. In total, 72 sampling cards were used per replication, amounting to 216 cards per treatment.

2.7. Data Collection and Processing

All histograms in this article are drawn in excel.

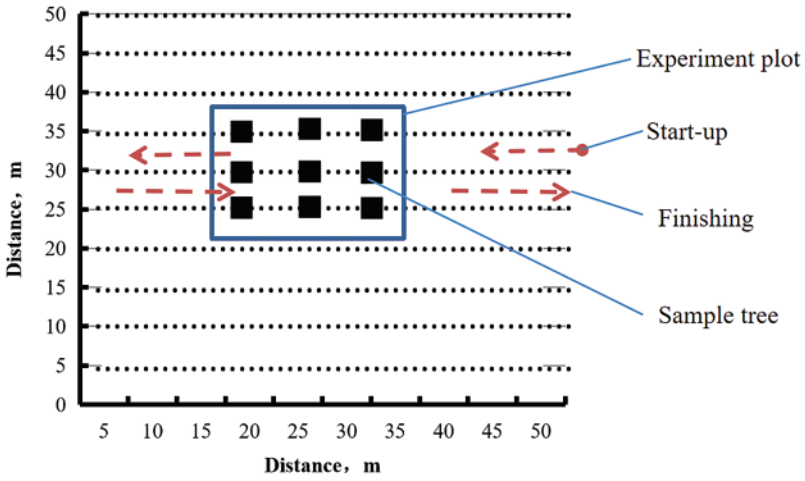

Fig. 3. Location layout of experimental cell.

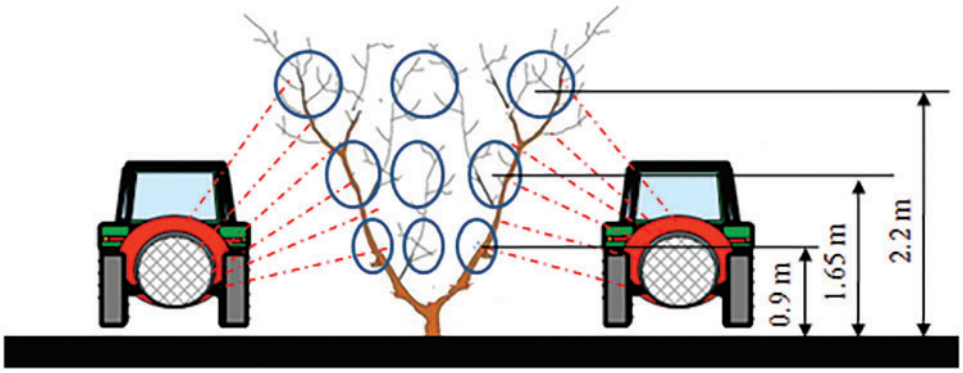

Fig. 4. Zone sampling strategies.

2.7.1. *Air Velocity*

The hot wire anemometers air velocity transducer (model 24-6111, kanomax company, Japan) was used to measure the air velocity at different spatial location. The air velocity contours was drawn by Surfer 8.0 (Golden Software company, USA) according to the dispersed measurement data.

2.7.2. *Droplets Density and Normalization*

The droplets deposition density was measured in the laboratory using a measuring software. The density was calculated according to the (3):

$$\rho = \frac{N}{S} \tag{3}$$

where ρ is the droplets density, dot/cm^2; N is the droplets number; S is the deposition area, cm^2;

In order to clarify the effect of tractor speed on droplet deposition and to keep the results consistent from one trial to another, all droplet densities were normalized to per unit volume according to the (4):

$$\rho_n = \frac{V_R}{V_S}\rho \tag{4}$$

where ρ_n is the normalized droplets density, dot/cm^2; V_R is tractor speed, m/s; V_S is reference speed, V_S was set equal to 0.7 m/s about walk speed. ρ is the testing droplets density, dot/cm^2.

2.7.3. *Coefficients of Variation (CV) of Droplet Density*

The coefficients of variation (CV) were used to evaluate the uniformity of distribution of droplets in the canopy of fruit tree and calculate according to the following formula:

$$CV - \frac{SD}{MN} \times 100\% \tag{5}$$

where SD is the standard deviation of the droplets density, dot/cm^2; MN is the average of the droplets density, dot/cm^2.

3. Results and Discussion

3.1. *Tree Morphology and Outlet Air Flow*

In this study, the pear trees were five years old, with a planting distance of 1 m and a row distance of 5 m. The Y-tree training system featured two branches positioned approximately 0.5 m from the ground, guiding the stems to grow upright along these branches. The top width of the 3-meter-high trees was about 4.5 m. The branches and stems were supported by steel tubes and steel wires, respectively.

To evaluate the canopy, the foliage area volume density (UL), which represents the total foliage area per unit volume, was used. The average canopy sizes were measured and are reported in Fig. 5. Due to winter pruning, the canopy was thinner along the stems, which are the primary fruit-bearing shoots. The average foliage area volume density for the interior and exterior zones was 1.51 m^{-1}

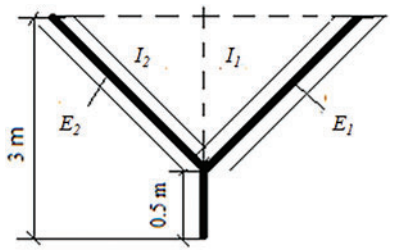

Fig. 5. Structure and parameters of the canopy.

TABLE III: Foliage Area Volume Density Evaluation

Sectors	E_1	I_1	I_2	E_2
U_L/m^{-1}	6.55	1.54	1.48	6.52

and 6.54 m^{-1}, respectively (Table III). This pruning system positively impacted photosynthesis.

Air velocity measurements were taken before the droplet deposition test. These measurements recorded exterior and interior initial air velocities of 25 m/s and 12.5 m/s, respectively. The air velocity contours (Fig. 6) indicated that the air velocity within the "Y" canopy ranged from 2 m/s to 4 m/s, which was sufficient to facilitate leaf movement and droplet penetration.

3.2. Canopy Average Droplet Density and Coefficients of Variation

Fig. 7 and Table IV present the average droplet density on both the exposed and hidden faces at four different tractor speeds tested in the experiment. The normalized droplet density on the exposed face increased with tractor speed, ranging from 175.3 dot/cm^2 at 0.34 m/s to 199.3 dot/cm^2 at 1.05 m/s. Conversely, the normalized droplet density on the hidden face decreased with increased tractor speed, from 52.6 dot/cm^2 at 0.34 m/s to 27.6 dot/cm^2 at 1.05 m/s. Despite these variations, the overall average droplet densities were 187 dot/cm^2 for the exposed face and 42.2 dot/cm^2 for the hidden face, which are considered effective for pest control.

To assess the impact of tractor speed on overall droplet density, the average droplet density values for the exposed and hidden faces were calculated and plotted in Fig. 8. The

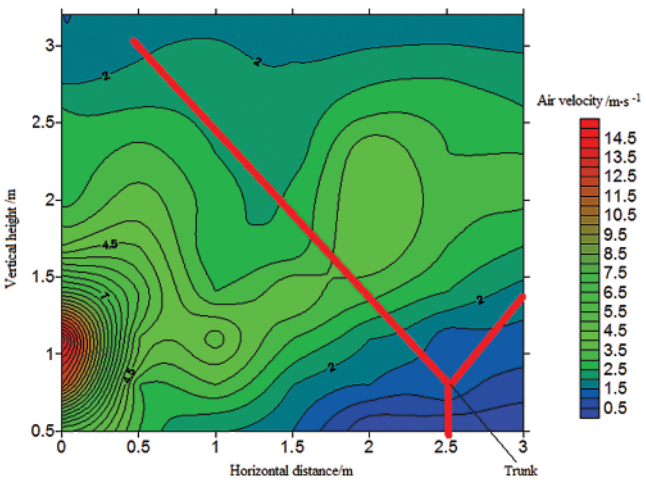

Fig. 6. The air velocity contours.

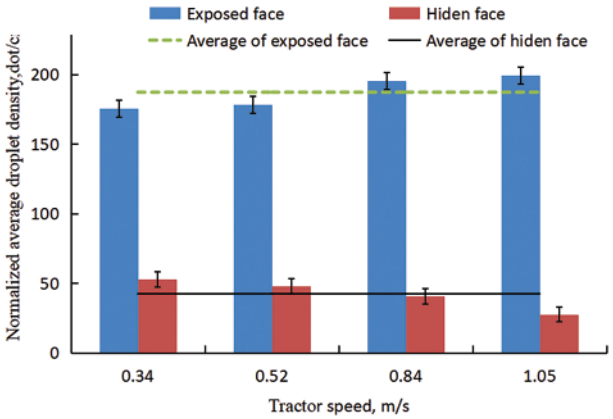

Fig. 7. Plots of normalized droplets density on exposed and hidden face.

normalized average droplet density across the four tractor speeds was approximately 114.6 dot/cm^2. The results indicate no significant difference in overall droplet density with changes in tractor speed.

The coefficients of variation (CV) for different treatments are reported in Table IV. The CV for the exposed face increased with tractor speed, rising from 47.8% at 0.34 m/s to 96% at 1.05 m/s. Tractor speed had no effect on the CV of the hidden face, which remained above 100%. The results suggest that the CV for the exposed face increased with electrostatic spraying, while the CV for the hidden face decreased. The average CV for both the exposed and hidden faces was calculated at 0.52 and 1.05 m/s, with and without the electrostatic system. The average CV decreased when the electrostatic system was activated, from 112.5% to 107.6% at 0.52 m/s and from 136% to 99.7% at 1.05 m/s.

3.3. Deposition Affected by Electrostatic System

To evaluate the deposition effect of electrostatic spray droplets on exposed face and hiden face. Droplet density of all samples in exposed face and hiden face were caculated respectively. The results were ploted in Fig. 9. which showed that the electrostatic spraying system had a signicant effect on hiden face deposition. The average droplet density on hiden face increased from 29.9 up to 38.2 dot/cm^2 (+29.4%). But the density on exposed face decreased from 201 to 190 dot/cm^2 (−5.4%). However, its effect was different between the exterior and interior zone. The overall average density of exposed and hidden face on exterior and interior zone were calculated respectively and ploted in Fig. 10. The increase in droplet deposition was located on the exterior zone, while decrease on interior zone. The normalized average droplet density on exterior zone increased from 122 up to 130 dot/cm^2. But the density on interior zone decreased from 101 to 91 dot/cm^2.

All the above results highlight that electrostatic spraying significantly affects the deposition on hiden face, especially on exterior zone. But the electrostatic system is not effect on charging droplet deposition on interior zone, because of the charging droplet can be attracted quickly by exterior canopy. Maybe the air velocity was not enough for transferring the charging droplet.

TABLE IV: Average Value (dot/cm^2) and CV of Droplet Density

Speed, m/s	Electrostatic system on				Electrostatic system off			
	Exposed face		Hidden face		Exposed face		Hidden face	
	Average value dot/cm^2	CV/%	Average value dot/cm^2	CV/%	Average value dot/cm^2	CV/%	Average value dot/cm^2	CV/%
0.34	175.3	47.8	52.6	106.5	–	–	–	–
0.52	176.6	59.4	48.3	155.9	183.8	51	36.3	174
0.84	195.5	83.8	40.7	155.3	–	–	–	–
1.05	199.3	96	27.6	103.4	218.2	80	23.6	192

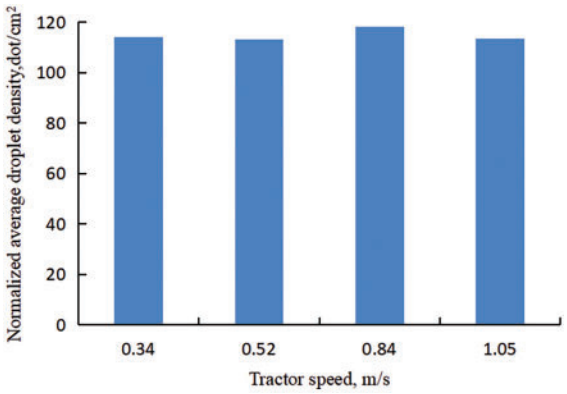

Fig. 8. Plots of average normalized droplets density at different four tractor speed.

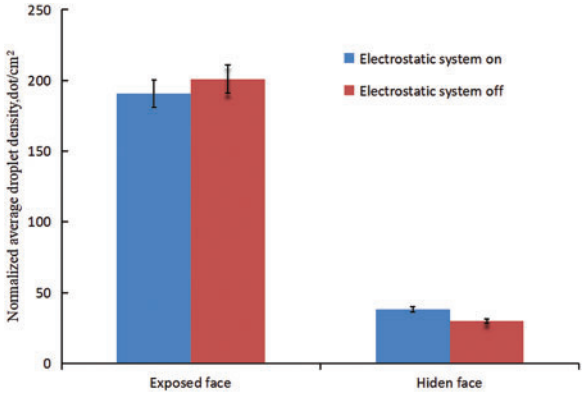

Fig. 9. Deposition on exposed and hidden face affected by electrostatic system.

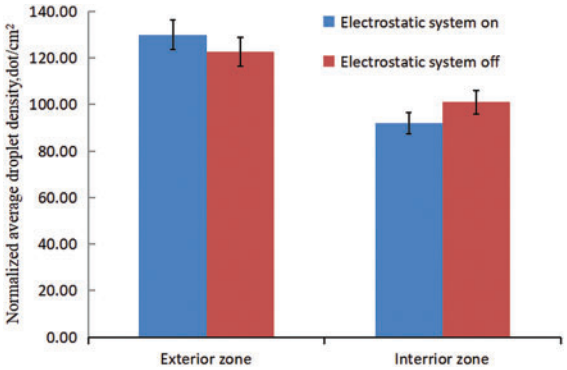

Fig. 10. Deposition on exposed and hiden face affected by electrostatic system.

4. Discussion

Electrostatic spraying technology offers high droplet deposition efficiency but is not widely adopted due to issues with application effectiveness, primarily related to short charge retention times and challenging application conditions. Further research should focus on the following areas:

1. *Optimization of Charging Parameters and Airflow:* Investigate how to better match charging parameters, spray airflow, and charged droplets to maximize the initial charge on droplets and ensure that they retain an effective charge upon reaching the target.
2. *Development of Operational Specifications:* Formulate detailed electrostatic spraying operation guidelines tailored to specific equipment to enhance the effectiveness of electrostatic spraying before widespread promotion.

5. Conclusion

1. *Tractor Speed and Droplet Density*: Tractor speed, ranging from 0.34 to 1.05 m/s, did not significantly affect overall droplet density. However, the density on the exposed face increased with tractor speed, while it decreased on the hidden face. The normalized average droplet density at all four tractor speeds was approximately 114.6 dot/cm^2.
2. *Effect of Electrostatic System:* The electrostatic system improved pesticide droplet deposition on the hidden face of leaves, particularly on the outer side of the fruit tree near the sprayer.
3. *Coefficient of Variation (CV):* The CV of droplet density on the exposed face increased with tractor speed, while tractor speed had no effect on the CV of the hidden face. Overall, the electrostatic system contributed to a reduction in CV.

Acknowledgment

This project is supported by independent innovation of agricultural science and technology of Jiangsu Province (Grant No. CX(22)3103); Research start-up Fund project of Nanjing Vocational University of Industry Technology (YK20-14-04); Jiangsu Province Precision Manufacturing Engineering and Technology Research Center.

Author Contributions

The authors confirm contribution to the paper as follows: study conception and design: Liangfu Zhou; data collection: Liangfu Zhou, Binbin Zhou; analysis and interpretation of results: Liangfu Zhou, Binbin Zhou; draft manuscript preparation: Liangfu Zhou; All authors

reviewed the results and approved the final version of the manuscript.

Conflict of Interest

The authors declare that they do not have any conflict of interest.

References

[1] Appah S, Wang P, Ou M, Gong C, Jia W. Review of electrostatic system parameters, charged droplets characteristics and substrate impact behavior from pesticides spraying. *Int J Agric Biol Eng*. 2019;12(2):1–9.
[2] Jing Z, Jianli S, Xiongkui H. Anti-drift performance experiment of Π-type recycling tunnel sprayer. *Trans CSAE*. 2012;43(4):37–9,125 (in Chinese with English abstract).
[3] Bashar S, Al-Kaisy HA, Al-Shroofy MN. Preparation of bio-composite coatings on titanium substrate by electrostatic spray deposition. *Key Eng Mater*. 2022;937:129–38.
[4] Mamidi VR, Ghanshyam C, Kumar PM. Electrostatic hand pressure knapsack spray system with enhanced performance for small scale farms. *J Electrostat*. 2013;71(4):785–90.
[5] Appah S, Zhou H, Wang P. Charged monosizeddroplet behaviour and wetting ability on hydrophobic leafsurfaces depending on surfactant-pesticide concentrate for mulation. *J Electrost*. 2019;100:103356.
[6] Wang S, He X, Song J, Zhang J. Charging and spraying performance test of bipolar contact electrostatic spraying system for unmanned aerial vehicle. *Trans Chin Soc Agric Eng*. 2018;34:82–9.
[7] Sarah HP, Lei L, Darrel D, Robert Z. Efficient electrospray deposition of surfaces smaller than the spray plume. *Nat Commun*. 2023;14(8):1–9.
[8] Angkawinitwong U, Courtenay AJ, Rodgers AM, Larraneta E, Williams GR. A Novel transdermal protein delivery strategy via electrohydrodynamic coating of PLGA microparticles onto microneedles. *ACS Appl Mater Interfaces*. 2020;12:12478–88.
[9] Salcedo R, Llop J, Campos J, Costas M, Gallart M, Ortega P, Gil E. Evaluation of leaf deposit quality between electrostatic and conventional multi-row sprayers in a trellised vineyard. *Crop Prot*. 2020;127:104964.
[10] Hu H, Kaizu Y, Huang J. Design and performance test of a novel UAV air-assisted electrostatic centrifugal spraying system. *Int J Agric Biol Eng*. 2022;15(5):7.
[11] Singh M, PGhanshyam C, Mishra PK. Current status of electrostatic spraying technology for efficient crop protection. *AMA Agric Mech Asia, Afr Lat Am*. 2013;44(2):46–53.
[12] Ming W, Shiqun D, Shichao L, Xiong M. Study on the effect of air-assisted spraying Auxiliary airflow on droplet size. *J Agric Mechanization Res*. 2024;46(10):192–7 (in Chinese with English abstract).
[13] Simone P, Emanuele C. Spray deposition in "tendone" vineyards when using a pneumatic electrostatic sprayer. *Crop Protec*. 2015;68(5):1–11.
[14] Pergher G, Lacovig A. Further studies on the effects of air flow rate and forward speed on spray deposition in vineyards. *VIII Workshop on Spray Application Techniques in Fruit Growing*, Barcelona, 2005.
[15] Cerruto E. Influence of airflow rate and forward speed on the spray depositon in vineyards. *J Agric Eng-Riv Ing Agrar*. 2007;1:31–8.
[16] Kwak D-B, Kim SC, Kuehn TH, David YHP. Quantitative analysis of droplet deposition produced by an electrostatic sprayer on a classroom table by using fluorescent tracer. *Build Environ*. 2021;205:108254.
[17] Liangfu Z, Ling Z, Xinyu X, *et al.* Design and experiment of 3WQ-400 double air-assisted electrostatic orchard sprayer. *Trans CSAE*. 2016;32(16):45–53 (in Chinese with English abstract).
[18] Müller V, Jobbagy M, Djurado E. Coupling sol-gel with electrospray deposition: towards nanotextured bioactive glass coatings. *J Eur Ceram Soc*. 2021;41:7288–300.
[19] Das A, Fehse S, Polack M, Panneerselvam R, Belder D. Surface-enhanced raman spectroscopic probing in digital microfluidics through a microspray hole. *Anal Chem*. 2023;95(2):1262–72.
[20] Appah S, Jia W, Ou M, Wang P, Gong C. Investigation of optimum applied voltage, liquid flow pressure, and spraying height-for pesticide application by induction charging. *Appl Eng Agric*. 2019;35:795–804.